# NEON ALGORITHM THEORETICAL BASIS DOCUMENT (ATBD):

# TIS SOIL HEAT FLUX


| PREPARED BY | ORGANIZATION | DATE |
|---|---|---|
| Natchaya Pingintha-Durden | SCI | 05/18/2016 |
| Josh Roberti | SCI | 05/18/2015 |
| Hank Loescher | SCI | 10/06/2012 |
| Edward Ayres | SCI | 10/06/2023 |



| APPROVALS | ORGANIZATION | APPROVAL DATE |
|---|---|---|
| Kate Thibault | SCI | 10/16/2023 |
| | | |

| RELEASED BY | ORGANIZATION | RELEASE DATE |
|---|---|---|
| Tanisha Waters | CM | 10/20/2023 |

See configuration management system for approval history.

The National Ecological Observatory Network is a project solely funded by the National Science Foundation and managed under cooperative agreement by Battelle. Any opinions, findings, and conclusions or recommendations expressed in this material are those of the author(s) and do not necessarily reflect the views of the National Science Foundation.

# Change Record

| REVISION | DATE | ECO # | DESCRIPTION OF CHANGE |
|---|---|---|---|
| A | 07/06/2016 | ECO-03910 | Initial Release |
| B | 02/05/2020 | ECO-06373 | Removed references to specific installation depths, calibration frequencies, and calibration durations, and noted that these are subject to change. Other minor text edits. |
| C | 04/20/2022 | ECO-06809 | • Update to reflect change in terminology from relocatable to gradient sites<br>• Added NEON to document title |
| D | 10/20/2023 | ECO-07046 | • Updated the method for identifying the start and end of sensor heating and the end of calibration period following changes to the timing of the L0 heater flag data.<br>• Removed the time regularization section. This method of regularization was unique to soil heat flux and now that the method for identifying the start and end of sensor heating and the end of calibration period has been updated the data can use the same regularization method as other NEON sensors. |

| | | | |
|---|---|---|---|
| | | | • Specified that the calibration heater flag (*F_H*) and calibration period flag (*F_Cal*) are assigned a value of -1 if the heater flag data are missing. |

TABLE OF CONTENTS



LIST OF TABLES AND FIGURES

# 1 DESCRIPTION

Contained in this document are details concerning soil heat flux measurements made at all NEON sites. Specifically, the processes necessary to convert "raw" sensor measurements into meaningful scientific units and their associated uncertainties are described.

## 1.1 Purpose

This document details the algorithms used for creating NEON Level 1 (L1) data products (DP) from Level 0 data, and ancillary data as defined in this document (such as calibration data), obtained via instrumental measurements made by Hukseflux HFP01SC: Self-Calibrating Heat Flux Sensor™ [NEON P/N: 0300260000]. It includes a detailed discussion of measurement theory and implementation, theoretical background, data product provenance, quality assurance and control methods used, assumptions, and a detailed estimation of uncertainty resulting in a cumulative uncertainty budget for this product.

## 1.2 Scope

The theoretical background and entire algorithmic process used to derive Level 1 data from Level 0 data for soil heat flux is described in this document. This document does not provide computational implementation details, except for cases where these stem directly from algorithmic choices explained here.

## 2 RELATED DOCUMENTS, ACRONYMS AND VARIABLE NOMENCLATURE

### 2.1 Applicable Documents

| | | |
|---|---|---|
| AD[01] | NEON.DOC.000001 | NEON OBSERVATORY DESIGN |
| AD[02] | NEON.DOC.011081 | NEON Algorithm Theoretical Basis Document (ATBD) - QA/QC Plausibility Testing |
| AD[03] | NEON.DOC.000783 | NEON Algorithm Theoretical Basis Document (ATBD) – Time Series Automatic Despiking for TIS Level 1 Data Products |
| AD[04] | NEON.DOC.000746 | Calibration Fixture and Sensor Uncertainty Analysis CVAL Uncertainty Manual) |
| AD[05] | NEON.DOC.000785 | TIS Level 1 Data Products Uncertainty Budget Estimation Plan |
| AD[06] | NEON.DOC.000779 | TIS Soil Plot Layout |
| AD[07] | NEON.DOC.001113 | NEON Algorithm Theoretical Basis Document (ATBD) – Quality Flags and Quality Metrics for IS Data Products |
| AD[08] | NEON.DOC.001069 | NEON Algorithm Theoretical Basis Document (ATBD) – Preprocessing for TIS Level 1 Data Products – QA/QC |

### 2.2 Reference Documents

| | | |
|---|---|---|
| RD[01] | NEON.DOC.000008 | NEON Acronym List |
| RD[02] | NEON.DOC.000243 | NEON Glossary of Terms |
| RD[03] | NEON.DOC.003223 | NEON Data Publication Workbook for TIS Soil Heat Flux Plate |

### 2.3 External References

External references contain information pertinent to this document but are not NEON configuration-controlled. Examples include manuals, brochures, technical notes, and external websites.

| | |
|---|---|
| ER [01] | HFP01SC Self Calibrating Heat Flux Sensor™ USER MANUAL HFP01SC Manual v0710 |
| ER [02] | Application and Specification of Heat Flux Sensors Version 9904 |
| ER [03] | Email correspondence with Jörgen Konings of Hukseflux (5 March 2014). N:\Science\FIU\TIS Assemblies\22. Soil Heat Flux\Other Design Docs_Notes\Email correspondence with Jorgen.pdf |

### 2.4 Acronyms

| **Acronym** | **Explanation** |
|---|---|
| AIS | Aquatic Instrument System |
| ATBD | Algorithm Theoretical Basis Document |

| | |
|---|---|
| CI | NEON Cyberinfrastructure |
| CVAL | NEON Calibration, Validation, and Audit Laboratory |
| DAS | Data Acquisition System |
| DP | Data Product |
| FDAS | Field Data Acquisition System |
| FIU | Fundamental Instrument Unit |
| GRAPE | Grouped Remote Analog Peripheral Equipment |
| Hz | Hertz |
| L0 | Level 0 |
| L1 | Level 1 |
| QA/QC | Quality assurance and quality control |
| TIS | Terrestrial Instrument System |

## 2.5 Variable Nomenclature

The symbols used to display the various inputs in the ATBD, e.g., calibration coefficients and uncertainty estimates, were chosen so that the equations can be easily interpreted by the reader. However, the symbols provided will not always reflect NEON's internal notation, which is relevant for CI's use, and or the notation that is used to present variables on NEON's data portal. Therefore, a lookup table is provided to distinguish what symbols specific variables can be tied to in the following document.

| Symbol | Internal Notation | Description |
|---|---|---|
| $E_C$ | CVALA0 | Original correction factor (V/Wm$^{-2}$) |
| $R_s$ | CVALA1 | Resistance of a current-sensing resistor in series with the film resistor (Ω) |
| $u_{A1}$ | U_CVALA1 | Combined, relative, calibration uncertainty provided in a database maintained and updated by CVAL (%) |
| $u_{A3}$ | U_CVALA3 | Combined, relative, calibration uncertainty (truth and trueness only); provided in a database maintained and updated by CVAL (%) |
| $u_{V1}$ | U_CVALV1 | Combined, relative Field DAS uncertainty for voltage measurements; provided in a database maintained and updated by CVAL (%) |
| $u_{V3}$ | U_CVALV3 | Combined, relative Field DAS uncertainty (truth and trueness only) for voltage measurements; provided in a database maintained and updated by CVAL (%) |
| $O_V$ | U_CVALV4 | Offset imposed by the FDAS for voltage readings provided in a database maintained and updated by CVAL (V) |

# 3 DATA PRODUCT DESCRIPTION

## 3.1 Variables Reported

The soil heat flux related L1 DPs provided by the algorithms documented in this ATBD are in RD[03].

## 3.2 Input Dependencies

**Table 1** details the soil heat flux related L0 DPs used to produce L1 DPs in this ATBD.

**Table 1.** List of soil heat flux related L0 DPs that are transformed into L1 DPs in this ATBD.

| Description | Sample Frequency | Units | Data Product Number |
|---|---|---|---|
| Soil heat flux sensor voltage ($V_S$) | 0.1 Hz | V | NEON.DOM.SITE.DP0.00040.001.01798.HOR.VER.000 |
| Calibration Heater flags (*F_H*) | 0.2 Hz | Binary (0/1) | NEON.DOM.SITE.DP0.00040.001.01799.HOR.VER.000 |
| Voltage across the current sensing resistor ($V_{cur}$) | 0.1 Hz | V | NEON.DOM.SITE.DP0.00040.001.01800.HOR.VER.000 |

## 3.3 Product Instances

The soil heat flux data product will be available at NEON core and gradient sites. At each core and gradient site, soil heat flux sensors will be distributed within three of the five soil plots within the TIS soil array. The HFP01SC sensor will be installed below the soil surface at a depth specified in the geolocation data. A description of how the sensors are located within the plots is described in AD[06].

## 3.4 Temporal Resolution and Extent

One- and thirty-minute averages of soil heat flux will be calculated to form L1 DPs.

## 3.5 Spatial Resolution and Extent

The soil heat flux measurement is spatially variable due to the small size of heat flux sensors relative to the scale of heterogeneity in surface conditions. A single measurement of soil heat flux is representative of the area of the sensor plate (Sauer and Horton, 2005). Therefore, replicate measurements are designed to be made across NEON's soil array. To maximize spatial coverage, soil heat flux sensors will be deployed in three out of five soil plots that comprise the soil array at each core and gradient site.

Their measurements will be representative of the soil at the point that the HFP01SC sensors are deployed.

# 4 SCIENTIFIC CONTEXT

Soil heat flux, typically accessed in the vertical direction, is the amount of thermal energy that moves by conduction across an area of soil in a unit of time and usually expressed in Watts per square meter (Sauer and Horton, 2005). Soil heat flux is a key parameter in surface energy balance studies. Typically, soil heat flux is measured a few centimeters below the soil surface rather than directly at the surface (Ochsner et al., 2007). Heat flux at the surface is obtained by summing the flux at the measurement depth and the change in heat storage in the soil layer above the measurement depth.

## 4.1 Theory of Measurement

A heat flux plate is the most common sensor to measure soil heat flux. Heat flux sensors are typically small, rigid, disc-shape sensors that are inserted horizontally into the soil at the reference depth (Ochsner et al., 2006). An encapsulated thermopile in the sensor produces a voltage proportional to the temperature gradient perpendicular (e.g., vertical) across the sensor body (Ochsner et al., 2006). The material of the heat flux sensor mimics the bulk density and thermal heat diffusivities of a common loam soil. Assuming that the actual soil heat flux is at steady state, i.e., the thermal conductivity of the body is constant and that the sensor has negligible influence on the thermal flow pattern, the output voltage is directly proportional to the local/measured heat flux, see **Figure 1**.

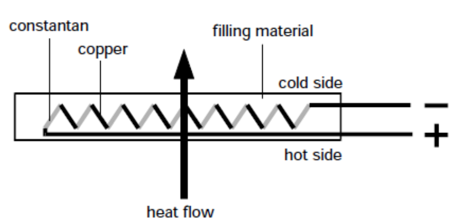


**Figure 1.** Conceptual schematic of a heat flux sensor (source: ER [02]).

Biases when using heat flux plates to measure soil heat flux can arise from both temperature differences and thermal conductivity differences between the sensor and soil. Typical heat flux sensors do not correct for this bias, as a result soil heat flux estimates are often under/overestimated (See Sections 6.1.1 through 6.1.3). The HFP01SC sensor self-calibrates using the Van den Bos-Hoeksema method to account, under empirical conditions, for these errors (ER [01]).

The HFP01SC sensor self-calibrates using the Van den Bos-Hoeksema method via a film heater mounted on top of the heat flux sensor. When the heater is activated, half of the heat flux would pass upward into the surrounding medium and half would pass downward through the plate. In an ideal case, the heat flux through the plate would be one half of the heating power. In reality, for a self-calibrating plate installed in soil, the actual flux through the plate caused by heating will generally not be equal to half of the heating power. The ratio of the ideal to actual flux is a measure of heat flow distortion during heating (Ochsner et al, 2006; ER [01]). The heat flow distortion during heating is then compared to the heat flow distortion under ambient conditions (measured when the heater is off) and is used to correct for the deflection error (Ochsner et al, 2006; ER [01]).

## 4.2 Theory of Algorithm

Given the caveats mentioned above, if the heat flux is assumed to be in a steady state, the signal of HFP01SC (in volt) is proportional to the local heat flux in W m$^{-2}$ (ER [01]). To perform a self-calibration and estimate the *in-situ* correction factor, the sensor will self-calibrate at regular intervals as defined in AD[05]. Self-calibration consists of applying 12 V to the film heater for 180 s to generate a heat pulse (**Figure 2**). The plate's response to the self-heating ($V_a$) is quantified by:

$$V_a = V_s(t_{180}) - \left(\left(\left(\frac{V_s(t_C) - V_s(t_0)}{t_C - t_0}\right) \cdot (t_{180} - t_0)\right) + V_s(t_0)\right) \qquad (1)$$

where:

$V_a$ = Sensor's response to self-heating (V)

$V_s(t_0)$ = Output from the sensor at start time of calibration period (V)

$V_s(t_{180})$ = Output from the sensor at 180 s after the initiation of heat pulse (V)

$V_s(t_C)$ = Output from the sensor at time *c* after the initiation of the heat pulse (signaling the end of a calibration period; V)

Note that the calibration interval was initially set to 3.25 h and subsequently changed to 13 h in 2020; however, this value is subject to further change. In addition, the duration of the entire calibration period ($t_C$) may be changed depending on soil type.

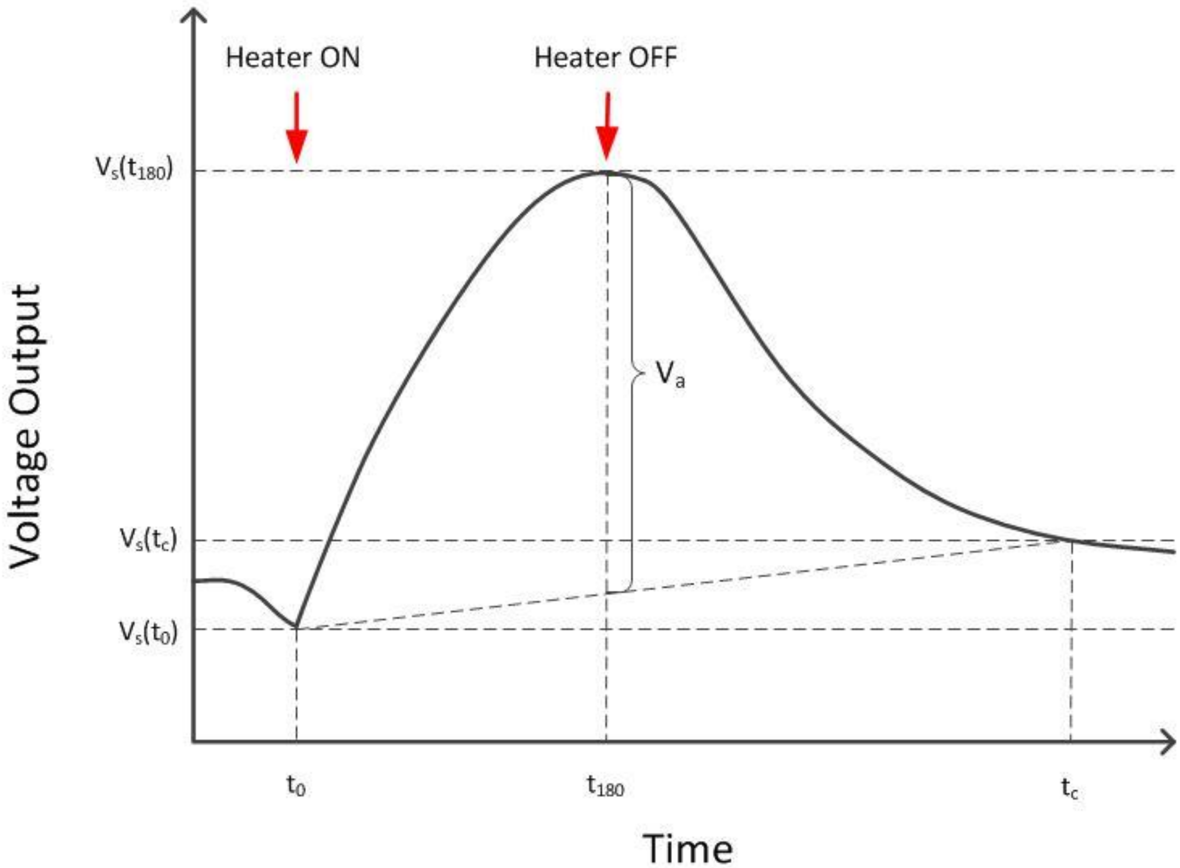


**Figure 2.** A conceptual plot of the voltage output ($V_s$) from the sensor when performing a self-calibration.

After the sensor response to self-heating ($V_a$) is obtained, the *in-situ* correction factor ($E_f$; V/Wm$^{-2}$) for the plate is then estimated as:

$$E_f = 2V_a \left[\frac{R_r^2 \, A_s}{V_{cur}^2 \, R_s}\right] \quad (2)$$

where: $R_r$ = Resistance of a current-sensing resistor in series with the film resistor (Ω; constant at 5 Ω)

$V_{cur}$ = Voltage across the current sensing resistor (V; output at 180 s after the initiation of heat pulse)

$A_s$ = Surface area of the plate (m$^2$; constant at 0.003885 m$^2$)

$R_s$ = Resistance of the film resistor (Ω)

The constant value of $R_r$ will be provided by ENG, while $A_s$ and $R_s$ is given by the manufacturer. These constant values will be provided by FIU and maintained in the CI data store. The *in-situ* correction factor is updated after every *in-situ* calibration.

Once the *in-situ* correction factor is resolved, soil heat flux can be determined by

$$\varphi = \frac{V_s}{E_f} \tag{3}$$

where:

$\varphi$ = soil heat flux (W m$^{-2}$)

$V_s$ = Output signal from the plate during measurement period (V)

$E_f$ = *In-situ* correction factor (V/Wm$^{-2}$)

After soil heat flux ($\varphi$) is determined, one-minute ($\varphi_{1min}$) and thirty-minute ($\varphi_{30min}$) averages will be determined accordingly to create L1 data products:

$$\varphi_{1min} = \frac{1}{n}\sum_{i=1}^{n}\varphi_i. \tag{4}$$

where, for each minute average, *n* is the number of measurements during the averaging period and $\varphi_i$ is 0.1 Hz soil heat flux measurement taken during the 60-second averaging period [0, 60). For a 1-minute average, $n$ = 6 if all data points are included, and

$$\varphi_{30min} = \frac{1}{n}\sum_{i=1}^{n}\varphi_i \tag{5}$$

where, for each thirty-minute average, *n* is the number of measurements during the averaging period - and $\varphi_i$ is 0.1 Hz soil heat flux measurement taken during the 1800-second averaging period [0, 1800).

Note: The beginning of the first averaging period in a series shall be the nearest whole minute less than or equal to the first timestamp in the series.

## 5 ALGORITHM IMPLEMENTATION

Data flow for signal processing of L1 data products will be treated in the following order.

1. Find all heater on and off events for the heater time series without regard to time regularization. To determine the start ($t_0$) and end ($t_{180}$) of heating during self-calibration the L0 heater data (*F_H*) is searched looking for instances where the heater turns on ($t_0$). For each instance, the heater off timestamp ($t_{180}$) is found by identifying the heater off readout that is more than 2 minutes 50 seconds after the heater on instant. The period [$t_0$, $t_{180}$) is then verified to be within 5 seconds of the expected heating period (180 s).
2. Once the heater on/off instances are identified, the soil heat flux sensor voltage ($V_s$) for $t_0$, $t_{180}$, and $t_c$ are found, along with the voltage across the current sensing resistor ($V_{cur}$) for $t_{180}$. The $V_s$ and $V_{cur}$ values must be within 10 seconds prior to $t_0$, $t_{180}$, and $t_c$, and are the ones closest to $t_0$, $t_{180}$, and $t_c$.
3. Assign the calibration heater flag (*F_H*) = '1' to 0.1 Hz data if the heater for *in-situ* self-calibration is turned on, *F_H* = '0' if the heater is off, or *F_H* = '-1' if the heater flag data is missing. The details are provided below.
4. Assign the calibration period flag (*F_Cal*) = '1' to 0.1 Hz data collected during the calibration period, *F_Cal* = '0' if outside the calibration period, or *F_Cal* = '-1' if the heater flag data is missing. The details are provided below.
5. During the calibration period, once the calibration heater is turned off, determine and assign the calibration heater quality flag (*QF_H*, i.e. '0' if the calibration heater is turned on correctly and '1' if the calibration heater failed to turn on) to 0.1 Hz data collected thereafter until the next *in-situ* self-calibration is performed. The *QF_H* will be determined using Eq. (6).
6. After all *in-situ* self-calibration processes are done, the *in-situ* correction factor will be determined according to Eq. (1) and (2).
7. Determine and assign the *in-situ* correction quality flag (*QF_EF*, i.e. '0' if there is no error and '1' if an error is detected during the calibration) to 0.1 Hz data collected thereafter until the next *in-situ* self-calibration is performed. The *QF_EF* will be determined using Eq. (7).
8. Soil heat flux (W $m^{-2}$) will be determined using Eq. (3) after regularizing the data according to AD[08]. The updated *in-situ* correction factor will be applied to the 0.1 Hz data collected thereafter until the next *in-situ* self-calibration is performed.
9. For the 0.1 Hz data that have *QF_EF* = '1' associated with its timestamp (i.e., indicating an error during the calibration), soil heat flux will be calculated using the original correction factor ($E_C$) given by the manufacturer.
10. Once the heating period is identified, the next heater on readout is identified, which completes the time period for the *in-situ* calibration, and the next in-situ calibration is calculated. If the next heater on event is found to be within the calibration period ($t_0$ to $t_c$), the calibration is marked with an error, as is the next one since the soil heat flux sensor voltage ($V_s$) at $t_0$ for the next calibration will be sampled during the cooling off period of the previous calibration. In

addition, the *in-situ* calibration expires after the time elapsed since the end of the calibration period exceeds the calibration interval (threshold defined in the CI data store; initially set to 3.25 hours and later changed to 13 hours).

11. QA/QC Plausibility tests will be applied to the data stream in accordance with AD[02]. The details are provided below.
12. Signal de-spiking and time series analysis will be applied to the data stream in accordance with AD[03].
13. One- and thirty-minute soil heat flux averages will be calculated using Eq. (4) and (5) and descriptive statistics (i.e. minimum, maximum, and variance) will be determined for both averaging periods.
14. Quality metrics, quality flags, and the final quality flag will be produced for one-, and thirty-minute averages according to AD[07]. However, for the following flags, *F_H, F_Cal, QF_H,* and *QF_EF,* if one or more of high flags ('1') are detected over the averaging period, set that flag to '1' for the whole averaging period.

**QA/QC Procedure**:

1. **Plausibility Tests** AD[02] – All plausibility tests will be determined for soil heat flux. Test parameters will be provided by FIU and maintained in the CI data store. All plausibility tests will be applied to the sensor's converted L0 DP and an associated pass/fail flag will be generated for each test. Note that the step test will not be run when the calibration period flag (*F_Cal*) is set high.
2. **Sensor test** – Flags will be generated for the sensor tests which include, the calibration heater flag (*F_H*), the calibration heater quality flag (*QF_H*), the calibration period flag (*F_Cal*), and the in-situ correction quality flag (*QF_EF*), which are defined below. These flags will be generated as part of the L1 data products and maintained in the CI data store. One- and thirty-minute averages of quality metrics of the these flags will be produced according to AD[07].
    a. Calibration heater flag (*F_H*) is derived from the L0 data products and is identified in the $C^3$ document (AD[05]). The calibration heater flag indicates the sensor is turned on to perform a self-calibration. The calibration heater flag shall read '0' under normal operating conditions and '1' when the sensor is self-calibrating. Any L0 DP (i.e., 0.1 Hz data) that has a calibration heater flag associated with its timestamp will not be used to compute soil heat flux (sensor's converted L0 DP).
    b. Calibration heater quality flag (*QF_H*) will be generated as part of the L1 data product to determine that the calibration heater is turned on correctly, *QF_H* = '0', and *QF_H* = '1'

when the calibration heater is failed to turn on. The calibration heater quality flag will be determined as follows:

$$QF\_H = \begin{cases} 1 \text{ if F\_H} = 1 \text{ and } [V_s(t_{180}) - V_s(t_0)] < \text{d} \cdot |V_s(t_c) - V_s(t_0)| \\ 0 \; otherwise. \end{cases} \tag{6}$$

where, d is the calibration heater quality flag threshold and set as default at 5.

Since the calibration heater quality flags are generated after the calibration heater is turned off, a specific calibration heater quality flag will be associated with the 0.1 Hz data collected after the preceding calibration heater quality flag.

c. Calibration period flag (*F_Cal*) will be generated as part of the L1 data product to indicate the calibration period for the sensor. The calibration period flag shall read '0' under normal operating conditions and '1'under calibration period. This period starts at the time the heater is turned on at $t_0$ and ends at $t_c$. Any L0 DP (i.e., 0.1 Hz data) that has a calibration heater flag associated with its timestamp will not be used to compute soil heat flux (sensor's converted L0 DP).

d. *In-situ* correction flag (*QF_EF*) will be generated as part of the L1 data product to indicate that an error occurred during the calibration process (i.e. '0' if there is no error and '1' if error is detected). Errors can arise in the *in-situ* calibration process if there is too much fluctuation between the heat flux in the soil during the calibration process (ER [01]). Since the *in-situ* correction quality flags are generated after *in-situ* self-calibration processes are done, a specific *in-situ* correction quality flag will be associated with the 0.1 Hz converted L0 DPs collected after the preceding *in-situ* correction quality flag. The *in-situ* correction quality flag will be determined as follows:

$$QF\_EF = \begin{cases} 1 \text{ if } E_f > (\text{a} * E_C) \text{ Or } E_f < (\text{b} * E_C) \text{ Or } |V_s(t_0) - V_s(t_c)| > \text{c}V_a \text{ Or } QF_H = 1 \\ 0 \; otherwise \end{cases} \tag{7}$$

where: $E_C$ = Original correction factor given by the manufacturer (provided by FIU and maintained in the CI data store; V/Wm$^{-2}$)

$a, b,$ and $c$ = *In-situ* correction quality flag thresholds; default value of $a = 1.20$, $b = 0.5$, and $c = 0.1$.

3. **Signal Despiking** – The time series despiking routine will be run according to AD[03]. Test parameters will be specified by FIU and maintained in the CI data store. Quality flags resulting from the despiking analysis will be applied according to AD[03]. Note that this test will not be run when the calibration period flag (*F_Cal*) is set high.
4. **Quality Flags (QFs) and Quality Metrics (QMs)** – If a datum has failed one or more of the following tests it will not be used to create a L1 DP: range, persistence, step, *F_H*, and *F_Cal*. α and β QFs and QMs will be determined using the flags listed in **Table 2**. In addition, L1 DPs will have a QA/QC report and quality metrics associated with each flag listed in **Table 2** as well as a final quality flag (*finalQF*), as detailed in AD[07]. Ancillary information needed for the algorithm and other information maintained in the CI data store is shown in **Table 3**.

**Table 2.** Flags associated with soil heat flux measurements.

| Tests |
|---|
| Range |
| Persistence |
| Step |
| Null |
| Gap |
| Signal De-spiking |
| Calibration period flag |
| *In-situ* correction flag |
| Alpha |
| Beta |
| Final Quality Flag |

**Table 3.** Information maintained in the CI data store for with soil heat flux measurements.

| Tests/Values | CI Data Store Contents |
|---|---|
| Range | Minimum and maximum values |

| **Tests/Values** | **CI Data Store Contents** |
| --- | --- |
| Persistence | Window size, threshold values and maximum time length |
| Step | Threshold values |
| Null | Test limit |
| Gap | Test limit |
| Signal Despiking | Time segments and threshold values |
| Uncertainty | AD[04] |
| Sensor Specifications | $R_r$ provided by ENG and $A_s$, $R_s$, and $E_C$ provided by the manufacture |
| Final Quality Flag | AD[07] |

# 6 UNCERTAINTY

Uncertainty of measurement is inevitable (ISO 1995; Taylor 1997). It is imperative that uncertainties are identified and quantified to determine statistical interpretations about mean quantity and variance structure; both are needed to construct higher level data products (i.e., L1 DP, etc.) and modeled processes. This portion of the document serves to identify, evaluate, and quantify sources of uncertainty relating to L1 soil heat flux DPs.

## 6.1 Uncertainty of Soil Heat Flux Measurements

Uncertainty of the soil heat flux assembly is discussed in this section. Sources of uncertainties include those arising from thermal conductivity (i.e., soil moisture) differences, temperature dependence, the sensor's self-calibration procedure, and measurement noise introduced by the data acquisition system. It should be noted that CVAL will not calibrate the soil heat flux sensors, as the sensors are programmed to conduct regularly scheduled self-calibrations (refer to Section 4.2).

### 6.1.1 Measurement Uncertainty

The following subsections present the uncertainties associated with *individual observations*. It is important to note that the uncertainties presented in the following subsections are *measurement uncertainties*, that is, they reflect the uncertainty of an *individual* measurement. These uncertainties should not be confused with those presented in Section 6.1.2.

NEON calculates measurement uncertainties according to recommendations of the Joint Committee for Guides in Metrology (JCGM) 2008. In essence, if a measurand *y* is a function of *n* input quantities $x_i$ $(i = 1, \dots, n)$, $i.e., y = f(x_1, x_2, \dots, x_n)$, the combined measurement uncertainty of *y*, assuming the inputs are independent, can be calculated as follows:

$$u_c(y) = \left(\sum_{i=1}^{N}\left(\frac{\partial f}{\partial x_i}\right)^2 u^2(x_i)\right)^{\frac{1}{2}} \tag{8}$$

where

$\frac{\partial f}{\partial x_i}$ = partial derivative of *y* with respect to $x_i$

$u(x_i)$ = combined standard uncertainty of $x_i$.

Thus, the uncertainty of the measurand can be found be summing the input uncertainties in quadrature.

#### 6.1.1.1 Thermal conductivity and temperature dependence

The thermal conductivity of the HFP01SC is 0.8 W $m^{-1}$ $K^{-1}$ (ER[01]), while that of soil can vary from 0.2 (dry) to 4.0 W $m^{-1}$ $K^{-1}$ (saturated). The discrepancy between the thermal conductivity of the soil heat flux sensor and that of the surrounding soil causes a thermal conductivity (or deflection) error. It is shown that this discrepancy can cause soil heat flux underestimates up to -16% of the expected measurement reading (ER[01]).

The HFP01SC is also prone to errors arising from temperature differences between the soil and the heat flux plate. These can be as large as ± 5% of the measurand if the sensor is left uncalibrated (ER[01]).

#### 6.1.1.2 In-situ self-calibration

Before a HFP01SC is shipped from Hukseflux to a customer, the sensor is calibrated to an ISO traceable "guarded hot plate." Once deployed in the field, the sensor is programmed to undergo self-calibrations at user-defined time intervals (See Section 4). If the sensor is successfully self-calibrated in the field, the thermal conductivity and temperature errors are corrected *to within ± 3% accuracy relative to the ISO traceable "guarded hot plate"* (ER[01]). This situation illustrates a pitfall, in that, the accuracy of soil heat flux measurements is quantified relative to a material that is not representative of soils. Because of this, the end-user should be cognizant that even in the event that the HFP01SC completes a successful in-situ self-calibration in the field, the resulting measurement uncertainty with respect to calibration is at minimum *± 3% accuracy relative to the ISO traceable "guarded hot plate."* This estimate is crude at best and is possibly underestimated relative to field conditions.

**Note:** Hukseflux uses the term *accuracy* to represent measurement *uncertainty*, and such values are given at 95% confidence throughout the manual (RD[05]).

To convert this expanded, relative uncertainty to an unexpanded, standard uncertainty, i.e., one that is given at a single confidence interval and is in units of measurement, Eq. (9) is used.

$$u_{CAL}(\varphi_i) = u_{A1} * \varphi_i \qquad (9)$$

Where,

$u_{CAL}(\varphi_i)$ = standard calibration uncertainty of an individual measurement (W $m^2$)

$u_{A1}$ = relative, calibration uncertainty provided in a database maintained and updated by CVAL (%).

$\varphi_i$ = individual, soil heat flux measurement (W $m^2$)

#### 6.1.1.3 Field DAS

The Field DAS (FDAS) introduces noise to the analog signals $V_s$ and $V_{cur}$. This uncertainty is quantified via:

$$u_{FDAS}(X_i) = (u_{V1} * X_i) + O_V \tag{10}$$

Where:

| | |
| --- | --- |
| $u_{FDAS}(X)$ | = standard uncertainty of the voltage measurement introduced by the Field DAS (V) |
| $X_i$ | = voltage measurement, either $V_s$, or $V_{cur}$ (V) |
| $u_{V1}$ | = combined, relative Field DAS uncertainty for voltage measurements provided in a database maintained and updated by CVAL (unitless) |
| $O_V$ | = offset imposed by the FDAS for voltage readings, provided by CVAL (V) |

The uncertainty introduced by the FDAS ultimately propagates to the soil heat flux measurement $\varphi$. Here, we detail this process in a few steps. First, we derive a combined uncertainty for $V_a$, which equals $f\left(V_s(t_0), V_s(t_{180}), V_s(t_c)\right)$.

The partial derivatives of the sensor's response to self-heating $V_a$, with respect to the appropriate voltage reading are:

$$\frac{\partial V_a}{\partial V_{s(t_C)}} = \frac{t_{180} - t_0}{t_0 - t_C} \tag{11}$$

$$\frac{\partial V_a}{\partial V_{s(t_0)}} = \frac{t_C - t_{180}}{t_0 - t_C} \tag{12}$$

$$\frac{\partial V_a}{\partial V_{s(t_{180})}} = 1 \tag{13}$$

The uncertainty of a voltage measurement $V_{s(t)}$, due to the FDAS is:

$$u_{FDAS_{V_{s(t)}}}(V_a) = \left|\frac{\partial V_a}{\partial V_{s(t)}}\right| u_{FDAS}\left(V_{s(t)}\right) \tag{14}$$

where:

$\frac{\partial V_{a_i}}{\partial V_{s(t)}}$ = partial derivative of Eq. (1) with respect to $V_{s(t)}$ (V)

$u_{FDAS_{V_{s(t)}}}(V_a)$ = standard uncertainty of measurement introduced by the Field DAS (V)

The combined uncertainty of $V_a$ is then:

$$u_c(V_a) = \left(u^2_{FDAS_{V_{s(t_0)}}}(V_a) + u^2_{FDAS_{V_{s(t_{180})}}}(V_a) + u^2_{FDAS_{V_{s(t_c)}}}(V_a)\right)^{\frac{1}{2}} \tag{15}$$

Next, the partial derivatives of the soil heat flux measurement $\varphi$, with respect to $V_s$, $V_{cur}$, and $V_a$ are derived. It should be noted that $V_s$ (Eq. (3)) and all $V_s(t)$ (Eq. (1)) are independent, as all $V_s(t)$ (Eq. (1)) are only valid during the calibration period, while measurements of $V_s$ (Eq. (3)) are only valid outside of the calibration period.

Substituting Eq. (2) into Eq. (3) and rearranging the terms we get:

$$\varphi = \frac{V_s}{E_f} = \frac{R_s V_{cur}^2 V_s}{2A_s R_r^2 V_a} \tag{16}$$

The partial derivatives of Eq. (16) with respect to $V_{cur}$, $V_a$, and $V_s$ are shown below.

$$\frac{\partial \varphi}{\partial V_{cur}} = \frac{R_s V_{cur} V_s}{A_s R_r^2 V_a} \tag{17}$$

$$\frac{\partial \varphi}{\partial V_s} = \frac{R_s V_{cur}^2}{2A_s R_r^2 V_a} \tag{18}$$

$$\frac{\partial \varphi}{\partial V_a} = -\frac{R_s V_{cur}^2 V_s}{2A_s R_r^2 V_a^2} \tag{19}$$

The partial uncertainties are thus:

$$u_{FDAS_{V_{cur}}}(\varphi_i) = \left|\frac{\partial \varphi}{\partial V_{cur}}\right| u_{FDAS}(V_{cur}) \tag{20}$$

$$u_{FDAS_{V_s}}(\varphi_i) = \left|\frac{\partial \varphi}{\partial V_s}\right| u_{FDAS}(V_{s_i}) \tag{21}$$

$$u_{FDAS_{V_a}}(\varphi_i) = \left|\frac{\partial \varphi}{\partial V_a}\right| u_c(V_a) \tag{22}$$

#### 6.1.1.4 Combined Measurement Uncertainty

The combined, standard, measurement uncertainty of an individual soil heat flux measurement $u_c(\varphi_i)$, given in units of W m$^{-2}$, is computed by summing the individual uncertainties in quadrature:

$$u_c(\varphi_i) = \left(u_{CAL}^2(\varphi_i) + u_{FDAS_{V_{cur}}}^2(\varphi_i) + u_{FDAS_{V_s}}^2(\varphi_i) + u_{FDAS_{V_a}}^2(\varphi_i)\right)^{\frac{1}{2}} \tag{23}$$

If the self-calibration process is unsuccessful (refer to Section 4.2), the errors mentioned in Section 6.1.1 can collectively over- or under-estimate measurements. In the event of an unsuccessful calibration, data will be flagged (*QF_EF*), and soil heat flux will be calculated using the original correction factor ($E_C$) given by the manufacturer. Uncertainty estimates will only comprise the manufacturer default uncertainty, $u_{CAL}(\varphi_i)$. The user should exercise caution when using any data where the manufacturer calibration coefficients are applied.

Given that the NEON Observatory will be monitoring both soil temperature and soil water content, it is theoretically possible to derive the thermal conductivity and temperature of the soil surrounding the heat flux sensor. Thus, if the self-calibration is unsuccessful, it may be possible to correct for the unavoidable errors caused by temperature and thermal conductivity discrepancies. This subject will need to be investigated in the future as NEON data are collected and analyzed.

#### 6.1.1.5 Expanded Measurement Uncertainty

The expanded measurement uncertainty is calculated as:

$$U_{95}(\varphi_i) = k_{95} * u_c(\varphi_i) \tag{24}$$

Where:

$U_{95}(\varphi_i)$ = expanded measurement uncertainty at 95% confidence ($W\ m^{-2}$)

$k_{95}$ = 2; coverage factor for 95% confidence (unitless)

### 6.1.2 Uncertainty of L1 Mean Data Product

The following subsections discuss uncertainties associated with temporally averaged, i.e., L1 mean, data products. As stated previously, it is important to note the differences between the *measurement uncertainties* presented in Section 6.1.1 and the uncertainties presented in the following subsections. The uncertainties presented in the following subsections reflect the uncertainty of a time-averaged mean value, that is, they reflect the uncertainty of a distribution of measurements collected under non-controlled conditions (i.e., those found in the field), as well as any uncertainties, in the form of *Truth* and *Trueness*, related to the accuracy of the field assembly.

#### 6.1.2.1 Repeatability (natural variation)

To quantify the uncertainty attributable to random effects, the distribution of the individual measurements is used. Specifically, the *estimated standard error of the mean (natural variation)* is computed. This value reflects the repeatability of insolation measurements for a specified time period:

$$u_{NAT}(\bar{\varphi}) = \frac{s(\varphi)}{\sqrt{n}} \tag{25}$$

Where,

$u_{NAT}(\bar{\varphi})$ = standard error of the mean (natural variation) (W $m^{-2}$)

$s(\varphi)$ = experimental standard deviation of individual observations for the defined time period (W $m^{-2}$)

$n$ = number of observations made during the defined time period. (unitless)

#### 6.1.2.2 Calibration

At NEON's CVAL, uncertainty budgets are partitioned by components of uncertainty, e.g., repeatability, reproducibility, and trueness. For many of NEON's L1 DP, the uncertainty resulting from sensor calibration that propagates to the L1 mean, DP is representative of measurement trueness and omits the repeatability and reproducibility. Repeatability and reproducibility of the L1 mean values are then quantified via the standard deviation of the mean (see Section 6.1.2.1). Unlike many of the sensors deployed throughout the NEON observatory, the soil heat flux sensors are not calibrated at NEON's CVAL before field deployment. The sensors are calibrated by Hukseflux and undergo self-calibrations once deployed in the field. Hukseflux does not provide individual estimates of trueness, repeatability, or reproducibility, rather, the vendor assigns an expanded uncertainty of ±3% to calibrated soil heat flux measurements (ER[01]). The *unexpanded* uncertainty provided by Hukseflux propagates to the combined uncertainty of the L1, mean DP.

$$u_{CAL}(\bar{\varphi}) = u_{A3} * \bar{\varphi} \tag{26}$$

Where,

| | |
|---|---|
| $u_{CAL}(\bar{\varphi})$ | = standard calibration uncertainty of a L1, mean, soil heat flux DP (W m$^2$) |
| $u_{A3}$ | = $u_{A1}$ (%) |
| $\bar{\varphi}$ | = L1, mean soil heat flux DP (W m$^2$) |

The decision to use the entire uncertainty estimate for the L1, mean data product can be philosophically debated. On one hand, it can be argued that this approach results in double-counting of repeatability and reproducibility. However, the magnitude of the natural variation of the L1, mean DP will most likely override the uncertainty estimate provided by Hukseflux. On the other hand, it can be argued that regardless of which term is propagated, i.e., measurement trueness only or the overall uncertainty, the uncertainty estimate provided by Hukseflux is most likely an underestimate of the uncertainty for the soil heat flux plate in soil (as opposed to the "guarded hot plate").

#### 6.1.2.3 Field DAS

Since the L1 mean soil heat flux DP is a function of the individual soil heat flux measurements, any measurement *bias* introduced by the Field DAS will be reflected in the L1 mean data product. Here, the raw measurements of $V_{cur}$ and $V_s$ that maximize the combined uncertainty of an individual measurement (Eq. (23)) are used in the calculation of the L1 mean DP uncertainty. Uncertainty components due to random effects, whether a function of the environment or the measurement assembly, are quantified via the natural variation of the mean (see Section 6.1.2.1).

The accuracy of the Field DAS in the form of *Truth* and *Trueness* propagates through to the uncertainty of the mean DP similarly to how the Field DAS uncertainties associated with a raw resistance and a raw voltage propagate through to the uncertainties of the measurement attributable to the Field DAS resistance and voltage readings.

$$u_{FDAS(TT)}(X_{MAX}) = (u_{V3} * X_{MAX}) + O_V \tag{27}$$

Where,

| | |
|---|---|
| $u_{FDAS(TT)}(X_{MAX})$ | = FDAS truth and trueness uncertainty of voltage measurement $X$ |
| $X_{MAX}$ | = measurements corresponding to the MAX index (V) |
| $u_{V3}$ | = relative, combined, Field DAS *Truth* and *Trueness* uncertainty for voltage measurements, provided by CVAL (unitless) |

Where, the subscript "$MAX$" represents the index, $i$, where the *maximum*, combined, standard, measurement uncertainty of an individual soil heat flux measurement is observed over a set (averaging period) of observations. Mathematically, this can be defined as:

$$MAX = \{i: u_c(\varphi_i) = \max[u_c(\varphi_1), \dots, u_c(\varphi_n)]\}. \tag{28}$$

Thus, from Eq. (20) through (21):

$$u_{FDAS(TT)_{V_{cur}}}(\bar{\varphi}) = \left|\frac{\partial \varphi}{\partial V_{cur}}\right| u_{FDAS(TT)}(V_{cur}) \tag{29}$$

**Note:** $V_{cur}$ is observed at 180 seconds after the initiation of heat pulse (during calibration cycle). As such, $V_{cur}$ from the most recent calibration cycle shall be used in Eq. (29)

$$u_{FDAS(TT)_{V_s}}(\bar{\varphi}) = \left|\frac{\partial \varphi}{\partial V_s}\right|_{V_{s_{MAX}}} u_{FDAS(TT)}\left(V_{s_{MAX}}\right) \tag{30}$$

where

$\left|\frac{\partial \varphi}{\partial V_{cur}}\right|$ = partial derivative of $\varphi$ with respect to $V_{cur}$ (Eq. (17); W m$^{-2}$ V$^{-1}$)

$\left|\frac{\partial \varphi}{\partial V_s}\right|_{V_{s_{MAX}}}$ = partial derivative of $\varphi$ with respect to $V_s$ (Eq. (18)) evaluated at $V_{s_{MAX}}$ (W m$^{-2}$ V$^{-1}$)

Because $V_s(t_0), V_s(t_{180})$, and $V_s(t_c)$ are measurements pertaining only to self-calibration, the bias of these measurements that is introduced by the DAS will be quantified during the calibration period and not when the maximum combined uncertainty of an individual measurement $\varphi_i$, is observed. Thus, the following equations are used:

$$u_{FDAS(TT)}\left(V_{s(t)}\right) = \left(u_{V3} * V_{s(t)}\right) + O_V \tag{31}$$

$$u_{FDAS(TT)_{V_{s(t)}}}(V_a) = \left|\frac{\partial V_a}{\partial V_{s(t)}}\right| u_{FDAS(TT)}\left(V_{s(t)}\right) \tag{32}$$

$$u_c(V_a) = \left(u^2_{FDAS(TT)_{V_{s(t_0)}}}(V_a) + u^2_{FDAS(TT)_{V_{s(t_{180})}}}(V_a) + u^2_{FDAS(TT)_{V_{s(t_c)}}}(V_a)\right)^{\frac{1}{2}} \tag{33}$$

$$u_{FDAS(TT)_{V_a}}(\bar{\varphi}) = \left|\frac{\partial \varphi}{\partial V_a}\right| u_c(V_a) \tag{34}$$

#### 6.1.2.4 Combined Uncertainty

The combined uncertainty for the L1, mean, soil heat flux data product, $u_c(\bar{\varphi})$, given in units of W m$^{-2}$, is computed by summing the uncertainties from Sections 6.1.2.1 through 6.1.2.3 in quadrature:

$$u_c(\bar{\varphi}) = \left(u_{CAL}^2(\bar{\varphi}) + u_{NAT}^2(\bar{\varphi}) + u_{FDAS(TT)_{V_{cur}}}^2(\bar{\varphi}) + u_{FDAS(TT)_{V_s}}^2(\bar{\varphi}) + u_{FDAS(TT)_{V_a}}^2(\bar{\varphi})\right)^{\frac{1}{2}} \quad (35)$$

In the event of an unsuccessful calibration, data will be flagged (*QF_EF*), and soil heat flux will be calculated using the original correction factor ($E_C$) given by the manufacturer. Uncertainty estimates will only comprise the manufacturer default uncertainty, $u_{CAL}(\varphi_i)$. The user should exercise caution when using any data where the manufacturer calibration coefficients are applied.

Note that the combined uncertainty of soil heat flux which calculated using the original correction factor given by the manufacturer will be computed by accounting the uncertainties from $u_{NAT}(\bar{\varphi})$ and $u_{CAL}(\bar{\varphi})$.

#### 6.1.2.5 Expanded Uncertainty

The expanded uncertainty is calculated as:

$$U_{95}(\bar{\varphi}) = k_{95} * u_c(\bar{\varphi}) \quad (36)$$

Where:

| | |
|---|---|
| $U_{95}(\bar{\varphi})$ | = expanded L1 mean data product uncertainty at 95% confidence (W m$^{-2}$) |
| $k_{95}$ | = 2; coverage factor for 95% confidence (unitless) |

### 6.2 Uncertainty Budget

The uncertainty budget is a visual aid detailing i) quantifiable sources of uncertainty, ii) means by which they are derived, and iii) the order of their propagation. Uncertainties denoted in this budget are either derived within this document or will be provided by other NEON teams (e.g., CVAL) and stored in the CI data store.

**Table 4.** Uncertainty budget for individual soil heat flux measurements. Shaded rows denote the order of uncertainty propagation (from lightest to darkest).

| **Source of measurement uncertainty** | **measurement uncertainty component $u(x_i)$** | **measurement uncertainty value [W m$^{-2}$]** | $\frac{\partial f}{\partial x_i}$ | $u_{x_i}(Y) \equiv \left\lvert \frac{\partial f}{\partial x_i} \right\rvert u(x_i)$ **[W m$^{-2}$]** |
|---|---|---|---|---|
| Soil heat flux | $u_c(\varphi_i)$ | Eq. (23) | n/a | n/a |
| Traceable calibration | $u_{CAL}(\varphi_i)$ | Eq. (9) | n/a | Eq. (9) |
| FDAS (signal) | $u_{FDAS}(V_{cur_i})$ | Eq. (10) [V] | Eq. (17) | Eq. (20) |
| FDAS (signal) | $u_{FDAS}(V_{s_i})$ | Eq. (10) [V] | Eq. (18) | Eq. (21) |
| In-situ cal. FDAS | $u_c(V_a)$ | Eq. (15) [V] | Eq. (19) | Eq. (22) |
| FDAS (signal) | $u_{FDAS}(V_s(t_0))$ | Eq. (10) [V] | Eq. (11) | Eq. (14) |
| FDAS (signal) | $u_{FDAS}(V_s(t_{180}))$ | Eq. (10) [V] | Eq. (12) | Eq. (14) |
| FDAS (signal) | $u_{FDAS}(V_s(t_c))$ | Eq. (10) [V] | Eq. (13) | Eq. (14) |

**Table 5.** Uncertainty budget for L1 mean soil heat flux DPs. Shaded rows denote the order of uncertainty propagation (from lightest to darkest).

| **Source of uncertainty** | **uncertainty component $u(x_i)$** | **uncertainty value [W m$^{-2}$]** | $\frac{\partial f}{\partial x_i}$ | $u_{u_{x_i}}(Y) \equiv \left\lvert \frac{\partial f}{\partial x_i} \right\rvert u(x_i)$ **[W m$^{-2}$]** |
|---|---|---|---|---|
| Soil heat flux | $u_c(\bar{\varphi})$ | Eq. (35) | n/a | n/a |
| Natural variation | $u_{NAT}(\bar{\varphi})$ | Eq. (25) | n/a | Eq. (25) |
| Traceable calibration | $u_{CAL}(\bar{\varphi})$ | Eq. (26) | n/a | Eq. (26) |
| FDAS (signal) | $u_{FDAS(TT)}(V_{cur\,MA}$ | Eq. (27) | Eq. (17) | Eq. (29) |
| FDAS (signal) | $u_{FDAS(TT)}(V_{s\,MAX})$ | Eq. (27) | Eq. (18) | Eq. (30) |
| In-situ cal. FDAS | $u_c(V_a)$ | Eq. (33) | Eq. (19) | Eq. (34) |
| FDAS (signal) | $u_{FDAS(TT)}(V_{s(t_0)})$ | Eq. (31) | Eq. (11) | Eq. (32) |
| FDAS (signal) | $u_{FDAS(TT)}(V_{s(t_{180})}$ | Eq. (31) | Eq. (12) | Eq. (32) |

| | | | | |
|---|---|---|---|---|
| FDAS (signal) | $u_{FDAS(TT)}\left(V_{s(t_c)}\right)$ | Eq. (31) | Eq. (13) | Eq. (32) |

## 7 FUTURE PLANS AND MODIFICATIONS

The frequency of self-calibrations (see AD[05]), time period of self-calibrations (see $t_c$ in Eq.(1)), calibration heater quality flag threshold (see $\mathrm{d}$ in Eq.(6)), and *in-situ* correction flag thresholds (see (see $\mathrm{a}$, $\mathrm{b}$, and $\mathrm{c}$ in Eq.(7)) may change to site-specific values.

Future system flags may be incorporated into the data stream and included in the QA/QC summary DP ($Qsum_{1min}$ and $Qsum_{30min}$) that summarizes any flagged data that went into the computation of the L1 DP.

## 8 REFERENCES

Joint Committee for Guides in Metrology (JCGM) (2008) Evaluation of measurement data – Guide to the expression of uncertainty in measurement. pp. 120.

JCGM (2012) International vocabulary of metrology – Basic and general concepts and associated terms (VIM). 3rd Edition. pp. 92

Ochsner, T.E., Sauer, T.J., and Horton, R. (2006) Field tests of the soil heat flux plate method and some alternatives. *Agronomy Journal*, **98**, 1005-1014.

Ochsner, T.E., Sauer, T.J., and Horton, R. (2007) Soil heat storage measurements in energy balance studies. *Agronomy Journal*, **99**, 311-319.

Sauer, T.J. and Horton, R. (2005) Soil heat flux. In Hatfield, J.L., and J.M. Baker (Eds). *Micrometeorology in Agricultural Systems*, Agronomy Monograph, **47**, pp. 131-154. Madison, Wisconsin, USA.

Taylor, J. R. (1997) An Introduction to Error Analysis: The Study of Uncertainties in Physical Measurements. University Science Books, Mill Valley, California.